*Optica Applicata, Vol. XXIV, No. 1–2, 1994*

# Vibrational kinetics of $CO_2$ molecules in gas discharge with high specific input power

R. Sh. Islamov, M. A. Kerimkulov, Yu. B. Konev, V. N. Ochkin, S. Yu. Savinov, A. P. Shotov, M. V. Spiridonov, I. I. Zasavitskii

Russian Academy of Science, P. N. Lebedev Physical Institute, Leninski Prospekt 53, Moscow, Russia.

Z. Trzęsowski

Military University of Technology, Institute of Quantum Electronics, ul. Kaliskiego 2, 01–489 Warszawa, Poland.

Investigations of active media of compact, waveguide $CO_2$ lasers having high specific energy parameters (exceeding by about two orders the corresponding power in common $CO_2$ lasers), and unique spectral characteristics, are indisputably of interest. The first-order approximations of the parameters of such lasers are usually obtained from the results of numerous investigations of the active media in wide tubes, under the premises that the gas discharges are similar. The output power calculated in such a way turned out to be appreciably larger (up to an order of magnitude) than the real one. Plasmochemical processes are assumed to play a large role. This fact results in an increased density of the oxygen atoms, which influence the relaxation of the asymmetric mode of $CO_2$, the presence of noticeable amounts of negative ions and redistribution of the electron density over the radius, and the presence of an ion component of the current. Systematic investigations of the distributions of $CO_2$ molecules over the vibrational-rotational levels at various laser mixture pressures and discharge currents are described in this paper. A theoretical analysis of vibrational kinetics of $CO_2$ moleculse was carried out on this basis.

## 1. Introduction

In view of the various applications of compact $CO_2$ lasers of the waveguide type ($CO_2$WG), having high specific energy parameters and unique spectral characteristics, investigations of their active media are indisputably of interests. The active element of such a laser is a discharge in a narrow tube of radius $R \sim 1$ mm, and the specific electric input power exceeds by about two orders the corresponding power in the wider ($R \sim 1$ cm) discharge channels of open-cavity $CO_2$ lasers.

The first-order approximation of the parameters of the active media of $CO_2$WG laser are frequently obtained from the results of numerous investigations of the active media in wide tubes, using the premises that gas discharges are similar although it is known that these premises are approximate [1]. More reliable predictions of $CO_2$WG parameters require special simulation. At the first stage it seemed most natural to use the known $CO_2$ laser design methods that have been well developed for traditional systems. However, the attempts made this way were not successful. The energy parameters calculated for $CO_2$WG with this procedure

turned out to be appreciably larger (up to an order of magnitude) than the real ones [2].

On the other hand, it is clear that, when calculated and measured lasing powers are compared, not only the characteristics of the active medium, but also those of the cavity and waveguide losses must be taken into account and such an analysis comprises separate complicated problems. Therefore, it is advantageous to separate these factors.

For the assessment to what extent the simulation of the processes in an active medium is possible, a comparison of the calculated and experimental distributions of the working molecules over the vibrational-rotational levels is of great interest.

Systematic investigations of the distributions of $CO_2$ molecules over the vibrational-rotational levels at various laser mixture pressures and discharge currents are described in this paper. A theoretical analysis of vibrational kinetics of $CO_2$ molecules was carried out on this basis.

## 2. Experimental conditions, procedure and technique

### 2.1. Measurement conditions

The active medium of a $CO_2$WAG laser operating on the mixture $CO_2-N_2-He$ (1:1:8) was investigated in a water-cooled discharge BeO ceramic capillary with the inside and outside diameters of $2R = 2$ and 6 mm. The total length of the tube was 60 mm and the length of the discharge region along the capillary axis was 50 mm. The gas pressure $P$ was 30–120 torr, and the discharge current $I$ was 2–10 mA dc. Kovar electrodes were led out through side stubs. There existed a weak gas flow whose consumption was determined from the rate of flow out of a container of known volume. The rate of gas flow through the discharge gas was $\sim 5$ m/s.

### 2.2. Research design and methods

The population of rotational-vibrational levels of $CO_2$ molecules was determined by diode laser spectroscopy. The layout of the spectrometer is described in [3].

This spectrometer provided the following characteristics:

- region of quasi-continuous wavelength tuning — $2200-2300\ cm^{-1}$
- typical rate of frequency retuning — $10^5\ cm^{-1}s^{-1}$
- ranges of continuous frequency tuning — up to $12\ cm^{-1}$
- spectral resolution — not worse than $10^{-3}cm^{-1}$
- operating speed of the recording system — $10^{-8}s$

To measure the electric field intensities from the ends of the capillary, probes were introduced along the discharge axis. They were wires with the insulation removed from the ends, 0.2 mm in diameter and 1 mm long. In the frequency interval of $2200-2300\ cm^{-1}$ about 1000 vibrational-rotational absorption lines and transitions were recorded. These transitions coupled more than 30 pairs of vibrational levels of $^{12}C^{16}O_2$ and 5 pairs of vibrational levels of $^{13}C^{16}O_2$ from all four vibrational modes of the molecules. The corresponding vibrational transitions pertain to sequence $v_1v_2^lv_3 \rightarrow v_1v_2^l(v_3+1)$. Typical line widths under the conditions

of our experiments amounted to $5 \times 10^{-3}$ cm$^{-1}$. Therefore, the required accuracy at which the frequency of the line centre was determined was $3 \times 10^{-3}$ cm$^{-1}$. The primary fit to the frequency scale was made with a monochromator of about $\sim 1$ cm$^{-1}$ accuracy. The next step was the comparison between the $CO_2$ experimental absorbing spectrum and the spectrum obtained by simulation. For a relative calibration of the frequency scale transmission spectra of germanium Fabry–Perot etalons with free spectral ranges of 0.1 and 0.033 cm$^{-1}$ were recorded.

The small diameter of the $CO_2$WG laser channel leads to definite difficulties in the localization of the radial zone of the measurements. In those cases when the diameter of the probing laser beam ($\sim 1$ mm) is comparable with the capillary diameter ($\sim 2$ mm), comparison with the calculations calls for reducing the measured averaged quantities to those on the discharge axis.

Numerical calculations (see, [4]) carried out in the range of the investigated conditions have shown that at a probing beam diameter of 1 mm the needed correction of the values of the rotational temperature amount to 4 ... 7% when the spectrum section with $j > 20$ is used. A similar correction for the vibrational temperature does not exceed 10%.

Since the real measurement accuracy for both rotational and vibrational temperatures was certain to be of order of 2%, control measurements were made in which the beam was collimated to 0.4 mm in the discharge zone. The measurements have fully confirmed the correctness of the reduction procedure [4].

## 3. Experimental results

For all fixed values of the gas pressure and the discharge current, measurements of the distributions of the $CO_2$ molecules over the vibrational and rotational levels were made. For each of the experimental conditions about 20–30 vibrational states were recorded. The range of rotational levels in each of the states was limited to $j < 100$. Such detailed investigations have guaranteed a high accuracy and reliability of the results. The results given below, unless especially stipulated, pertain to a discharge in a BeO capillary.

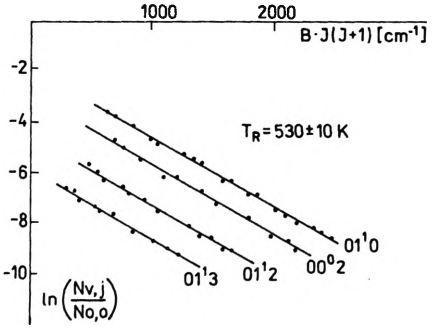


Fig. 1. Rotational population distribution for various vibrational levels. Gas mixture $CO_2$:$N_2$:He = 1:1:8, pressure $p = 60$ torr, discharge current $I = 9$ mA

Figure 1 shows in semilog scale examples of molecule distributions over rotational levels for four vibrationsl levels: $01^10$, $00^02$, $01^12$, $01^13$ at a pressure of 60 torr and current $I = 9$ mA. The rotational temperatures for all the vibrational levels were $530 \pm 10$ K. On general physical considerations, the rotational temperature was identified with the gas temperature, $T_R = T_G$. The measured gas temperatures *vs.* the discharge current and gas pressure are summarized in Fig. 2. Figure 3 shows the analogous dependencies for strength $E$ of axial electric field.

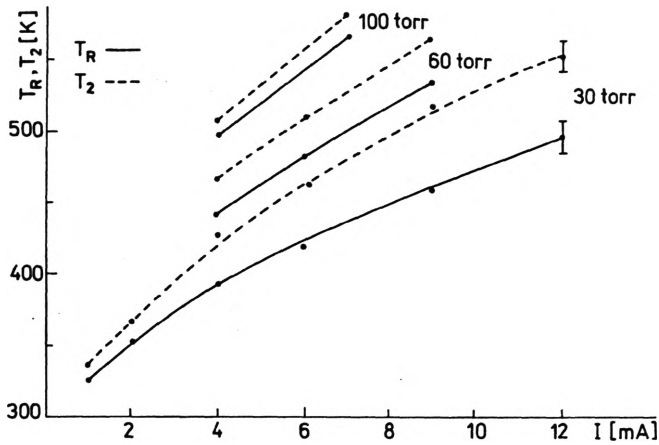


Fig. 2. Rotational temperature $T_R$ (solid line) and vibrational temperature $T_2$ (dotted line) *vs.* discharge current. Gas pressure $p = 30$, 60 and 100 torr

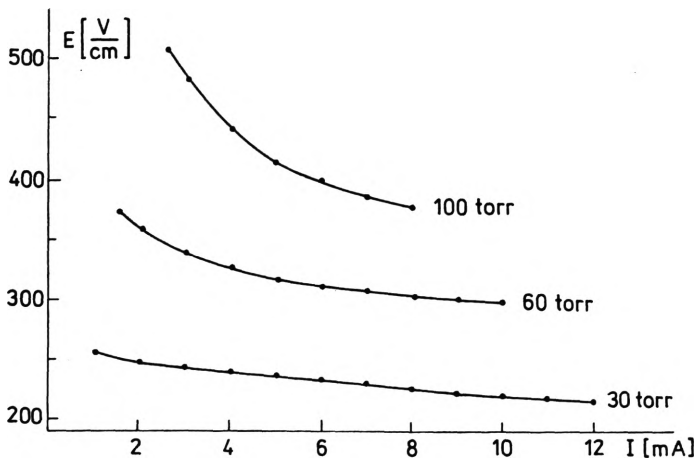


Fig. 3. Axial electric field in the positive column of capillary discharge *vs.* discharge current. Gas pressure $p = 30$, 60 and 100 torr

A typical example of the distribution of the $CO_2$ molecules over the vibrational levels from different vibrational modes at $I = 9$ mA and $p = 60$ torr is shown in Fig. 4.

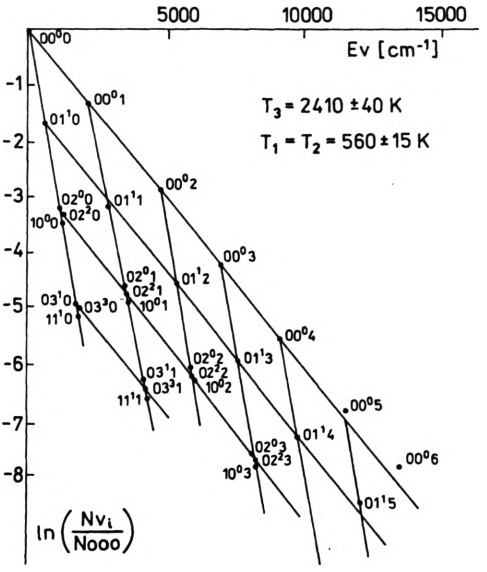


Fig. 4. Vibrational population distribution in the $CO_2$ molecules. Gas mixture $CO_2$:$N_2$:He = 1:1:8, pressure $p = 60$ torr, discharge current $I = 9$ mA

In this case, the data are on the population of the 31 vibrational level. Vibrational temperatures were: for asymmetric mode $T_3 = 2140 \pm 40$ K, for deformational and asymmetric mode $T_1 = T_2 = 560 \pm 15$ K. The measured vibrational temperatures are summarized in Fig. 2 and Fig. 5.

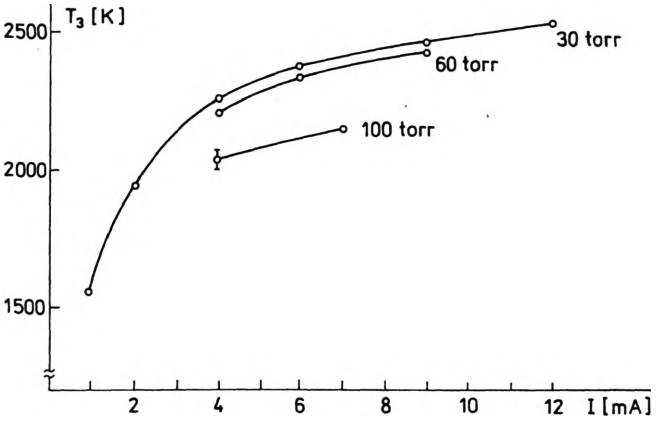


Fig. 5. Vibrational temperature $T_3$ *vs.* discharge current. Gas pressure $p = 30$, 60 and 100 torr

Knowing the gas vibrational-rotational distributions and temperature, we can also determine the total density of the molecules [3] from measurements of the absorption coefficient. This yields, in particular, information on the degree of dissociation of the working molecules in the discharge.

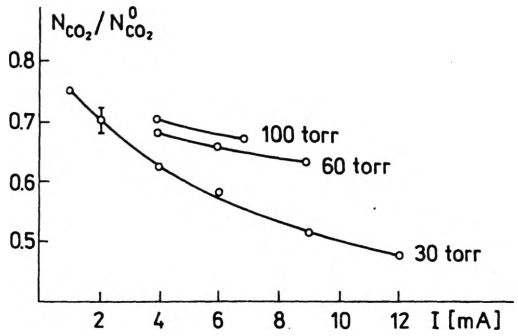


Fig. 6. Disssociation level of the $CO_2$ molecules *vs.* discharge current. Gas pressure $p = 30$, 60 and 100 torr

The dependence of $N_{CO_2}/N^0_{CO_2}$ ($N^0_{CO_2}$ is the density of the $CO_2$ molecules in the initial gas mixture at the real gas temperature) on the discharge conditions at various pressures, is shown in Fig. 6.

## 4. Discussion of results

### 4.1. Model of calculation of vibrational distributions

To calculate the populations of the vibrating levels of the molecules both the level-by-level approach and the vibrational temperature approaches were used. Just as in [5], the transitional description of the kinetics of $CO_2$ in the vibrational temperature approximation was preserved only for joint energy relaxation of the coupled (symmetric and deformation) modes.

The populations of the vibrational levels of $N_2$ and of the asymmetric mode of $CO_2$ are obtained by solution of the system of Boltzmann equations for the populations of individual molecules levels. Since the system of equations for interacting harmonic oscillators is well known (see, *e.g.*, [6]), but unwieldy, we present it in a symbolic form

$$\frac{dN_V}{dt} = R_V^{eV} + R_V^{VV} + R_V^{VT} + R_V^{D} \tag{1}$$

where the terms on the right-hand side are the rates of change of the populations of the corresponding levels by such processes as excitation by electron impact, VV exchange, VT relaxation, and diffusion. The constants of the VV and VT processes were assumed to be proportional to the square of the matrix element of the interaction operator and adiabaticity function, which depends on the energy defect $\Delta E$ of the process, the temperature, and the parameter $U_m$ of the colliding molecules. Just as in [7], [8] we used the adiabaticity function $F_M(\Delta E)$ obtained in [33] under the rather general assumptions

$$F_M(\Delta E) = A_M\left(\frac{\Delta E}{2kT}\right)\exp(-U_m|\Delta E|) \tag{2}$$

where $U_m$ is an undetermined parameter,

$$A_M(x) = \begin{cases} (x/2)^3 K_3(x)\exp(x) & \text{for } M \equiv CO_2,\ N_2\ CO \\ x^2/2K_2(x)\exp(x) & \text{for } M \equiv He,\ Ar,\ O \end{cases}$$

($K_n(x)$ is a modified Bessel function of order $n$ and $A_M(O) = 1$).

Such a parameter $U_m$ was chosen that the constants used in the calculation describe known constants of two processes of the same type with substantially different energy defects $\Delta E$ in the temperature region of interest to us. Thus, analysis of the constants of fast VV exchange in the reactions

$$CO_2(10^01)+CO_2(00^00) \rightarrow CO_2(10^00)+CO_2(00^01),$$
$$CO_2(00^01)+CO_2(01^10) \rightarrow CO_2(00^00)+CO_2(01^01)$$

obtained by quantum-mechanical calculations [34] allows us to express the rate constants of the VV exchange in an asymmetric mode in the form

$$k_{CO_2}^{CO_2\{v\rightarrow v-1;\ v\rightarrow v+1\}} = v(v+1)\cdot 6.96\cdot 10^6 (300/T)^{1.38} A_M(\Delta E/2kT)$$
$$\times \exp\left\{-\frac{3.99(T/300)^{0.54}|\Delta E|}{kT}\right\} s^{-1}\cdot torr^{-1}. \tag{3}$$

The analysis shows that this equation also describes well the behaviour of the constant $k_{CO_2}^{CO_2\{1\rightarrow 2;\ 1\rightarrow 0\}}$ obtained in the same reference. The results of [34] on the constants of the VV exchange between $N_2$ and the asymmetric mode of $CO_2$ yield

$$k_{N_2}^{CO_2\{v\rightarrow v-1;\ v\rightarrow v+1\}} = v(v+1)182\cdot 10^4 (300/T)^{1.31} A_M(\Delta E/2kT)$$
$$\times \exp\left\{-\frac{1.146|\Delta E|}{kT}\right\} s^{-1} torr^{-1}. \tag{4}$$

The currently available data on the VV exchange constant in nitrogen differ several times. The data from [9] was used in the calculation. The temperature dependence and the multiplier in the adiabaticity factor correspond to the theoretical results [10] for the constants $k_{N_2(0\rightarrow 1)}^{N_2(1\rightarrow 0)}$ and $k_{N_2(8\rightarrow 9)}^{N_2(1\rightarrow 0)}$

$$k_{N_2}^{N_2\{v\rightarrow v-1;\ v\rightarrow v+1\}} = v(v+1)3.2\cdot 10^3 (300/T)^{0.5} A_M(\Delta E/2kT)$$
$$\times \exp\left\{-\frac{2.1(T/300)^{0.58}|\Delta E|}{kT}\right\} s^{-1} torr^{-1}. \tag{5}$$

The relaxation constants $k_M^{10}$ of the lower vibrational levels $N_2$ and $CO_2$ are known for a wide range of temperatures [11], [12]. The same adiabaticity factor (2) was used in the anharmonicity term in the calculation of the detailed constants of VT relaxation in the $N_2$ and in the asymmetric mode of $CO_2$

$$k_M^{v\rightarrow v-1} = vk_M^{10} A_M(\Delta E^V/2kT)/A_M(\Delta E^1/2kT)$$
$$\times \exp\left\{-\frac{U_m}{2kT}(|\Delta E^V| - \Delta E^1)\right\} s^{-1} torr^{-1}. \tag{6}$$

Since the VT relaxation of the asymmetric vibrations $CO_2(00^0v)$ proceeds via excitation of the levels $(11^1v-1)$ and $(03^1v-1)$ [11], the energy defect $\Delta E$ was determined and used in analogous equation as for VT relaxation of $N_2$ in collisions with the $CO_2$ molecules. For lack of direct data on the influence of the energy defect on the VT relaxation constants, the parameter $U_m$ was assumed to be the same as in Eqs. (3), (4) and (5) for the corresponding collision partners. The values of $U_m$ for helium atoms was assumed to be the same as for the process (4).

Vibration energy exchange between the molecules CO and $CO_2$ and $N_2$ is considerably slower than between $CO_2$ and $N_2$. Because the CO density under our conditions is relatively small, the vibrational excitation of CO can be taken into account within the framework of the vibrational temperatures method. The corresponding rate constants are given in [13]–[16].

In Equation (1), the term $R_M^{eV}$ that describes pumping by electrons includes excitation of vibrational levels by electron impact both from the ground state and from lower lying levels.

The procedure for calculating the kinetic coefficients and energy balance of electrons in mixtures containing vibrationally excited $CO_2$ molecules is described in [17], [18]. The cross-sections for excitation of the first eight vibrational levels of the $N_2$ molecules from the ground state were taken from [19] and, in conjunction with the results of [20], used to determine the cross-sections of steplike processes.

Relaxation of vibrationally excited $CO_2$, CO, and $N_2$ molecules on the walls of a tube of radius $R$ was assumed to be given by

$$R_V^D = k^D(N_V - N_V^T). \tag{7}$$

To estimate $k^D$ data from the review [35] and the proper equation within the boundary conditions on the wall were used

$$(k^D)^{-1} = D_V^{-1}\left(\frac{R}{2.405}\right)^2 + \left(\frac{\varepsilon}{2-\varepsilon}\frac{c}{R}\right)^{-1} \tag{8}$$

where $D_V$ is the diffusion coefficient of the vibrationally excited molecules, $\varepsilon$ is the accomodation coefficient of the vibrational energy of the molecules, $c = (8\ kT/\pi m)^{1/2}$ is the average thermal velocity of molecules of mass $m$, $N_V^T$ is the equilibrium population of the level. When solving the vibrational kinetics equation (1), it was assumed that the quanta reaching the upper level of $N_2$ either from the asymmetric mode of $CO_2$ in the VV exchange process or upon excitation by electrons, are removed from the system as a result of fast relaxation. Altogether, 30 levels both for $N_2$ and $CO_2$ were taken into account.

### 4.2. Comparison of calculation with experiment

The high specific input electric power typical of $CO_2$ waveguide lasers calls for an analysis of the validity of the theoretical approach based on the known vibrational temperatures approximation. Therefore, we have carried out a level-by-level examination and comparison of the calculated and experimental results on the discharge axis. The values of $E/N$ and gas temperature used in the calculations were

taken from experiment, and the influence of chemical reaction products was disregarded in the first stange.

Table 1 shows the experimental and calculated results for 11 different conditions in the pressure range of 30–100 torr and for currents of 1–12 mA. All the results pertain to the axis of BeO discharge capillary. In the first three columns there are listed the pressure, discharge current, and relative axial-field strength $E/N$. These are followed by the pump-power density on the tube axis 4, measurements of the degree of $CO_2$ dissociation in the discharge 5, and the gas temperature 6. In columns 7 and 8 there are given the values of the vibrational temperatures $T_2$ of the deformation mode (the experimental values of $T_2$ in all the investigated cases were equal to the vibrational temperature $T_1$ of the symmetric mode) and $T_3$ of the asymmetric mode. Both the experimental and calculated values of $T_2$ and $T_3$ are listed. In columns 9 and 10 there are shown the values of the rate constants $K_2$ and $K_3$ of relaxation of the deformation and asymmetric modes. Each lower value pertains to a mixture having the initial composition and it has been obtained by the procedure described in Sec. 4.1. These conditions yield those calculated values of $T_2$ and $T_3$ that are indicated in the lower lines in columns 7 and 8. The upper lines contain those values of $K_2$ and $K_3$, which give the best agreement between the calculated and measured vibrational temperatures.

It can be seen from Table 1 that, in order to attribute the measurement results to relaxation of vibrational modes in the entire range of conditions, it is necessary to increase the relaxation rate constants by 1, 2 ... 5 times. In our opinion, such strong discrepancies may be caused by the influence of the plasmochemical transformations on the rates of the excitation processes and the deactivation of the molecular vibrations in the plasma.

### 4.3. Influence of chemical transformation products on the relaxation rates

The real chemical composition of the plasma of $CO_2$WG lasers with dc excitation was investigated in a number of studies and is known well enough. The change of the composition from the initial is due mainly to $CO_2$ dissociation. The supplementary components are CO, $O_2$ and O. Both CO and $O_2$ influence insignificantly the VT relaxation constants $K_2$ and $K_3$. On the contrary, it is known that the oxygen atoms are quite active in the quenching of asymmetric vibrations of $CO_2$. The corresponding rate constant is $(6.7\pm1.2)10^3\,s^{-1}\,torr^{-1}$ [21], [22]. At a 1% concentration in the mixture, the contribution of the oxygen atoms to the relaxation is approximately equal to the contribution of all the remaining components. The presence of noticeable amounts of oxygen atoms is a distinct feature of $CO_2$WG lasers compared with traditional $CO_2$ lasers with wide tubes, owing to the substantially higher current density. This circumstance was pointed out already in [24]. It appears that the rate of CO relaxation on O atoms is approximately the same [23] (measurements were made only at temperatures higher than 1500 K). The relaxation rate of $N_2$ on O atoms is slower by about one order [23].

Table 1

| 1 | 2 | 3 | 4 | 5 | 6 | 7 | 8 | 9 | 10 |
|---|---|---|---|---|---|---|---|---|---|
| $p$ [torr] | $I$ [mA] | $E/N$ $10^{-16}$ Vcm$^2$ | $W$ [W/cm$^3$] | $\frac{P_{CO_2}}{P_{CO}+P_{CO_2}}$ | $T_R = R_0$ [K] | $T_2$ experim. / theor. [K] | $T_3$ experim. / theor. [K] | $K_2$ fit. / theor. 10 /s torr | $K_3$ fit. / theor. 1/s torr |
| | | | | | | 335 | 1550 | 1740 | 228 |
| 30 | 1 | 2.8 | 18 | 0.25 | 325 | 367 | 2094 | 332 | 88 |
| | | | | | | 365 | 1930 | 1920 | 268 |
| 30 | 2 | 3.0 | 36 | 0.30 | 350 | 419 | 2592 | 367 | 90 |
| | | | | | | 425 | 2250 | 1450 | 344 |
| 30 | 4 | 3.2 | 70 | 0.37 | 390 | 494 | 2990 | 423 | 98 |
| | | | | | | 460 | 2350 | 1600 | 458 |
| 30 | 6 | 3.3 | 102 | 0.42 | 415 | 547 | 3230 | 459 | 103 |
| | | | | | | 515 | 2420 | 1650 | 584 |
| 30 | 9 | 3.5 | 146 | 0.47 | 455 | 611 | 3510 | 521 | 116 |
| | | | | | | 545 | 2510 | 2290 | 664 |
| 30 | 12 | 3.6 | 186 | 0.51 | 490 | 669 | 3702 | 564 | 131 |
| | | | | | | 465 | 2200 | 1290 | 257 |
| 60 | 4 | 2.5 | 95 | 0.32 | 440 | 502 | 3029 | 494 | 128 |
| | | | | | | 505 | 2340 | 1900 | 322 |
| 60 | 6 | 2.6 | 136 | 0.34 | 480 | 559 | 3328 | 550 | 132 |
| | | | | | | 560 | 2410 | 2230 | 415 |
| 60 | 9 | 2.7 | 196 | 0.36 | 530 | 628 | 3648 | 620 | 155 |
| | | | | | | 505 | 2030 | 1890 | 225 |
| 100 | 4 | 2.2 | 128 | 0.3 | 495 | 526 | 2686 | 572 | 140 |
| | | | | | | 580 | 2130 | 1940 | 353 |
| 100 | 7 | 2.7 | 196 | 0.33 | 565 | 609 | 3274 | 668 | 173 |

The density of the oxygen atoms was determined under similar conditions by mass spectrometric [24]–[26] and spectral [27] methods. In the region where the experimental conditions coincide, the results of these investigations are in satisfactory agreement.

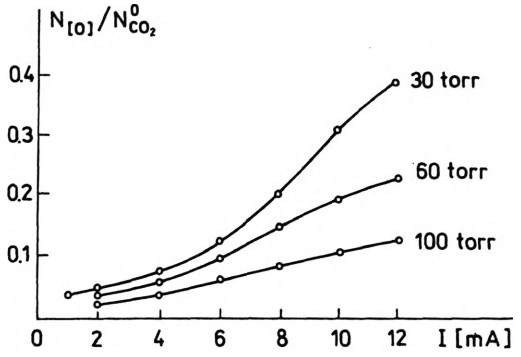


Fig. 7. Concentration of the O atoms on capillary axis *vs.* discharge current, gas mixture: $CO_2$:$N_2$:He = 1:1:8, pressure $p$ = 60 torr [27]

The inset of Figure 7 shows the changes, obtained by interpolation of the results of [27], of the ratio of the density of the oxygen atoms to the density of the $CO_2$ molecules in the initial mixture of the real gas in the discharge with change of the discharge conditions. This data as a percentage of the total particle density is also shown for convenience in Table 2

Table 2.

| $p$ [torr] | | | | 30 | | | | 60 | | | 100 |
|---|---|---|---|---|---|---|---|---|---|---|---|
| $I$ [mA] | 1 | 2 | 4 | 6 | 9 | 12 | 4 | 6 | 9 | 4 | 7 |
| $N_0/N$ [%] | 0.3 | 0.5 | 0.8 | 1.3 | 2.9 | 3.8 | 0.6 | 1.0 | 170 | 0.4 | 0.65 |
| $\Delta K_3^0$ | 20 | 34 | 54 | 87 | 164 | 255 | 40 | 67 | 114 | 27 | 44 |
| $K_3^{theor.}+\Delta K_3^0$ | 108 | 124 | 152 | 190 | 280 | 386 | 168 | 199 | 269 | 167 | 217 |

The table shows also the values of $\Delta K_3^0$. These values should be added to the calculated constant $K_3^{calc}$ to take into account the influence of the oxygen atom, and their sum is $K_3^{calc}+\Delta K_3^0$. Comparison of Table 1 and 2 shows that allowance for relaxation on oxygen atoms makes the summary constant $K_3^{calc}+\Delta K_3^0$ larger than the fitting constant $K_3^{fit}$. Thus, allowance for the influence of the oxygen atoms on the acceleration of the vibrational VT relaxation makes it possible to make the calculation and experimental results closer, although the difference remains as significant as before.

### 4.4. Influence of plasmochemical processes on the spatial distribution of the pump power density

As it is always done in calculations of traditional $CO_2$ lasers with wide tubes, the rate of excitation of molecular oscillations was determined from the measured total discharge current and field intensity, and under the assumption of Bessel radial distributions of the current and electron densities. It is commonly known that the Bessel ditribution follows from the Schottky theory of the positive column of a glow discharge. The theory is based on the assumption that ambipolar diffusion prevails over the bulk recombination and that the charged component of the plasma consists of electrons and positive ions. However, if the plasma contains electronegative particles, it is possible in principle to have intense formation of negative ions and their accumulation in amounts exceeding the electron density.

The theory of the positive column in electronegative gases was considered in many papers (see [29], [30] and the citation therein). The main qualitative result is that under certain conditions, the electron density can be distributed over the radius much more uniformly than over a Bessel function. In this case, the pump power density on the discharge axis will be lower than for a Bessel distribution.

Arguments and estimates of this kind are confirmed by the results of a paper [31], in which an open microwave cavity was used to investigate a discharge in a capillary of 2 mm diameter under conditions close to ours. It was established that in the range of 20–60 torr the fraction of the ion current is ~15% and the radial profile of the electron density deviates noticeably from a Bessel one (see Fig. 8).

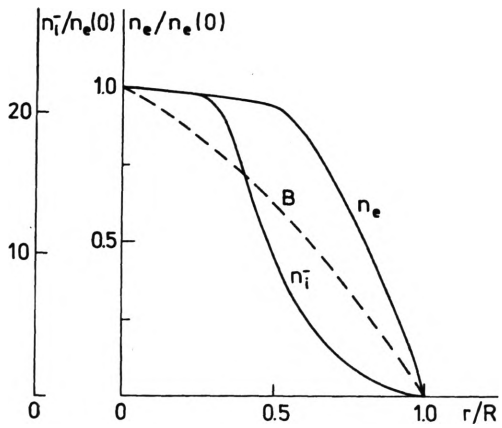


Fig. 8. Radial distribution of the negative ions concentration in the positive discharge column in gas mixture: $CO_2$:$N_2$:He:Xe = 1:1:8:0.3 at pressure $p > 20$ torr [31]. B – Bessel profile, $n_e$ – electrons concentration, $n_i$ – negative ions concentration

An estimate, based on the experimental data, of the effective datachment constant leads to a value $k \approx 1.5 \cdot 10^{-14}\,\mathrm{cm^3\,s^{-1}}$. If such rate constants given above are assumed, the transition to the regime of accumulation of negative ions should take place in this composition of the gas components at a pressure > 20 torr.

Using the experimental results of [31], we calculate that the electron-pump power on the capillary axis is smaller by 1.5 times than it would be for a Bessel profile and in the absence of an ion current.

Table 3 gives comparison of the experimental data and calculated temperatures of $T_3$. The table shows also the values of $K_3$.

Figure 9 shows the experimental and calculated dependencies of the temperature $T_3$ on the discharge current at pressures of 30, 60 and 100 torr for the discharge axis. In the final calculation we took into account the quenching of the oscillations by the hydrogen atoms and the deviation of the radii profile from a Bessel one. One can see a satisfactory agreement between the calculation and the experiment. The discrepance between them is no more than 6%.

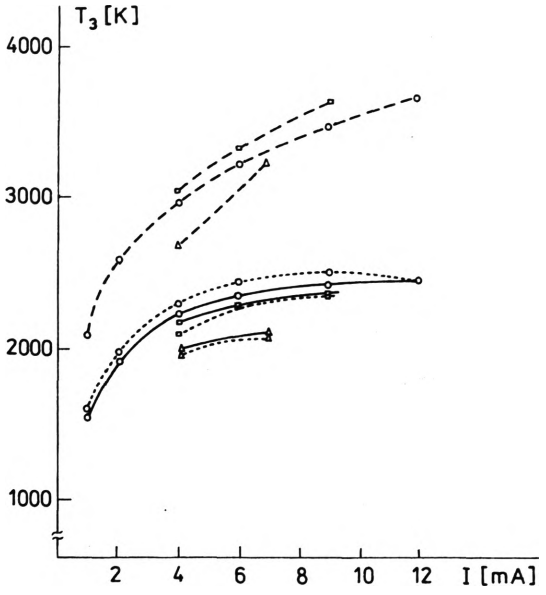


Fig. 9. Vibrational temperature $T_3$ *vs.* discharge current. Gas pressure $p$ = 30 (○), 60 (□) and 100 (△) torr. Solid line – experimental results, dashed line – calculated value (without correction), dotted line – calculated value (with correction)

For the sake of clarity of the initial calculation results, the two, above mentioned factors, shown in the same figure, are not taken into account. We have noted (Tab. 1) considerable discrepancies between the calculated VT relaxation constants of a block of symmetric and deformation modes of $CO_2$, on the one hand, and the constants needed for fitting to the experiment, on the other. Here the strongest relaxator in the mixture is helium, which constitutes 80% of the mixture, and the presence of small amounts of oxygen atoms cannot influence substantially the relaxation rate. Allowance for the influence of negative ions on the electron component (decrease of the pump power on the axis) make its possible to reconcile almost completely the calculated and experimental values of $T_2$ when the calculated values of the

Table 3

| 1 | 2 | 3 | 4 | 5 | 6 | 7 | 8 | 9 |
|---|---|---|---|---|---|---|---|---|
| $p$ [torr] | $i$ [mA] | input data | | after correction | | $T_3^{theor}$ [K] | $T_3^{theor}$ [K] | $T_3^{theor}$ [K] |
| | | $K_3^{theor}$ | $K_3^{fit}$ | $K_3^{theor}$ | $K_3^{fit}$ | input date | | correction |
| 30 | 1 | 88 | 228 | 108 | 119 | 2094 | 1550 | 1600 |
| 30 | 2 | 90 | 268 | 124 | 140 | 2592 | 1930 | 1990 |
| 30 | 4 | 98 | 344 | 152 | 185 | 2990 | 2250 | 2330 |
| 30 | 6 | 103 | 458 | 190 | 252 | 3230 | 2350 | 2480 |
| 30 | 9 | 116 | 584 | 280 | 329 | 3510 | 2420 | 2520 |
| 30 | 12 | 131 | 664 | 386 | 386 | 3702 | 2510 | 2510 |
| 60 | 4 | 128 | 257 | 168 | 149 | 3029 | 2200 | 2100 |
| 60 | 6 | 132 | 322 | 199 | 197 | 3328 | 2340 | 2330 |
| 60 | 9 | 155 | 415 | 269 | 240 | 3648 | 2410 | 2320 |
| 100 | 4 | 140 | 225 | 167 | 160 | 2686 | 2020 | 2000 |
| 100 | 7 | 173 | 353 | 217 | 210 | 3274 | 2130 | 2100 |

relaxation rate constants are used. It must be noted, however, that attainment of this agreement is not as instructive for $T_3$. The point is that the kinetic calculations make it possible to determine only the difference between the gas and vibrational temperatures, which is large for $T_3$ and small for $T_2$. In experiments, on the other hand, the gas and vibrational temperatures are measured separately with an error of 2–3%. Since in our range of conditions the deviation of vibrational temperature in the symmetric and deformation modes from the gas temperature is 5–15%, the error in the experimental determination of this discrepance can exceed 50%. We note at the same time that these errors do not influence too strongly the results of calculation of laser parameters, because of the low population, described by the temperature $T_2$, of lower laser levels.

## 5. Conclusions

The performed experimental investigations and simulation of the kinetic processes allow us to reveal circumstance that is substantial for understanding the difference between the descriptions of the active media of traditional cw $CO_2$ lasers with wide tubes and $CO_2$ waveguide lasers. The main cause is the higher specific energy input to the gas density in the case of waveguide lasers with capillary discharges, where plasmochemical processes assume a larger role. This fact results in an increased density of the oxygen atoms, which influence the relaxation of the asymmetric mode of $CO_2$, the presence of noticeable amounts of negative ions and the redistribution of the electron density over the radius, and the presence of an ion component of the current. Formation of negative cluster ions takes place in three-particle reactions, and the effect of the growth of their concentration is quadratic in the gas density. This effect and a number of other factors impose certain restrictions on the prediction of laser parameters by using, for the gas discharges, similarity relations that assume dominance of bimolecular reactions, ensuring invariance of the Boltzmann and Pauli equations under scale transformations [1]. At the same time, the results of the present study show that the use of numerical calculations based on traditional schemes and supplemented by notions concerning the specifics of plasmochemical processes make it possible to construct an adequate kinetic model of similar systems.

## References

[1] Abrams R. L., *Waveguide Lasers, Laser Handbook*, Vol. 8, North-Holland, Amsterdam 1979.

[2] Konev Yu. B., Lipatov N. I., Pashinin P. P., Prokhorov A. M., Kvantovaya Elektron. **11** (1984), 1641 (in Russian).

[3] Demyanenko A. V., Zasavitskii I. I., Ochkin V. N., Savinov S. Yu., Kvantovaya Elektron. **14** (1987), 851 (in Russian).

[4] Zasavitskii I. I., Islamov P. Sh., Kerimkulov M. A., Konev Yu. B., Ochkin V. N., Savinov S. Yu., Sobolev N. N., Spiridonov M. V., Shotov A. P., Preprint FIAN, No. 18, Moscow 1988 (in Russian).

[5] Pivovar V. A., Zh. Tekh. Fiz. **51** (1981), 1876 (in Russian).

[6] Dolinina V. I., Oraevskii A. N., Suchkov A. F., Urin B. M., Shebeko Yu. N., Zh. Tekh. Fiz. **48** (1978), 983 (in Russian).
[7] Blauer J. A., Zelazny S. W., Hager G. R., Solomon W. C., IEEE J. Quantum Electron. **15** (1979), 602.
[8] Islamov R. Sh., Konev Yu. B., PMTF, No. 4 (1985), 9 (in Russian).
[9] Valanskii S. I., Vereshchagin K. A., Volkov A. Yu., Pashinin P. P., Smirnov V. V., Fabelinskii V. I., Kholts L., Kvantovaya Elektron. **11** (1984), 1836 (in Russian).
[10] Billing G. D., Fisher E. R., Chem. Phys., Part 1, **18** (1976), 225; Part 2, **43** (1979), 395.
[11] Losev S. A., *Gazodinamicheskie lazery*, (in Russian) [Ed.] Nauka, Moscow 1971.
[12] Islamov R. Sh., Konev Yu. B., Lipatov N. I., Pashinin P. P., Preprint FIAN, No. 113, Moscow 1982 (in Russian).
[13] Roser W. A., Sharma D. R., Jr., Gerry E. T., J. Chem. Phys. **54** (1971), 1196.
[14] Starr D. F., Hancock J. K., J. Chem. Phys. **63** (1975), 4730.
[15] Taine J., Lepoutre F., Louis G., Chem. Phys. Lett. **58** (1978), 611.
[16] Allen D. C., Simpson C. J. S. M., Chem. Phys. **45** (1980), 203.
[17] Islamov R. Sh., Konev Yu. B., Lipatob N. I., Pashinin P. P., Preprint FIAN, No. 50, Moscow 1982 (in Russian).
[18] Islamov R. Sh., Konev Yu. B., *Proc. 15th ICPIG*, Minsk, Conf. Papers, Part 1., s. 1, s.a., p. 71.
[19] Shulz G. J., Phys. Rev. A **135** (1964). 988.
[20] Chen J. C. Y., J. Chem. Phys. **40** (1964), 3513.
[21] Buchwald W. I., Wolga G. I., J. Chem. Phys. **62** (1975), 2828.
[22] Cramp J. H. W., Lambert J. D., Chem. Phys. Lett. **22** (1973), 146.
[23] Gershenzon Yu. M., Nikitin E. E., Rozenshtein V. B., Umanskii S. Ya., Khimiya Plazmy (in Russian), [Ed.] B. M. Smirnov, 5 edition, Atomizdat, Moscow 1978, p. 3.
[24] Volchenok V. I., Komarov V. N., Ochkin V. N., Khimicheskaya fizika, No. 8 (1982), 1061 (in Russian).
[25] Volchenok V. I., Komarov V. N., Ochkin V. N., Khimiya vysokikh energii **18** (1984), 477 (in Russian).
[26] Volchenok V. I., Ochkin V. N., Simonov A. P., Khimiya vysokikh energii **20** (1984), 557 (in Russian).
[27] Zheenbaev N. Sh., Mamytbekov M. Z., Otorbaev D. K., Zh. P. S. **51** (1989), 12 (in Russian).
[28] Lowke J. J., Phelps A. U., Irwin B. W., J. Appl. Phys. **44** (1973), 4664.
[29] Ferreira C. M., Gousset G., Toureau M., J. Phys. D **21** (1988), 1403.
[30] Tsendin L. D., Zh. T. F. **59** (1989), 21 (in Russian).
[31] Smirnov A. S., Frolov K. S., Zh. T. F. **58** (1988), 1878 (in Russian).
[32] Nighan W. L., Wiegand W. J., Phys. Rev. A **10** (1974), 922.
[33] Procacci J., Levin R. D., J. Chem. Phys. **63** (1975), 4261.
[34] Pack R. T., J. Chem. Phys. **72** (1980), 6140.
[35] Gershenzon Yu. M., Nikitin E. E., Umanskii S. Yu., *Khimiya plasmy* (in Russian), [Ed.] B. M. Smirnov, 4 edition, Atomizdat, Moscow 1977, p. 61.

*Received April 5, 1994*